Krill defecation at depth reduces carbon flux attenuation in the Weddell Sea euphotic zone

Authors: Florence Atherden[1], Emily Rowlands[1], Gareth Flint[1], Sophie Fielding[1], Katrin Schmidt[2], Elaine Fileman[3], Maren Richter[4], Bethany Wilkinson[3], Angus Atkinson[3], Clara Manno[1]

1. British Antarctic Survey, Cambridge, UK
2. University of Plymouth, Plymouth, UK
3. Plymouth Marine Laboratory, Plymouth, UK
4. University of East Anglia, UK

Corresponding authors: Florence Atherden, flrden19@bas.ac.uk, Clara Manno, clanno@bas.ac.uk

Abstract

The Weddell Sea, Southern Ocean, is a highly productive location of deep-water formation and a globally important site of carbon sequestration. Here, the biological carbon pump is dominated by carbon-rich particulates which are both actively and passively transported to deep water (e.g. zooplankton faecal pellets and phytoplankton detritus). However, climate driven changes in sea ice have the potential to disrupt these processes, highlighting a need for contemporary observations. This study quantified the flux of particulate organic carbon (POC) and nitrogen (PON) across three depths (50, 100 ,150 m) at five locations (including shelf, off shelf, ice covered and ice-free environments) in the western Weddell Sea using a drifting sediment trap. POC and PON fluxes were greater on shelf than off-shelf, likely reflecting increased nutrient supply and productivity on shelf. No strong patterns between sea ice and ice-free stations were present, likely because the ice pack was constantly shifting, with most sites influenced by sea ice. The POC flux remained stable or increased with depth at most stations, ranging from 42.5 - 364.1 mg C m^{-2} day^{-1} (mean of 123.2 mg C m^{-2} day^{-1}). Krill faecal pellets represented 98% of all pellets, which contributed an estimated 17-99 % (median of 48 %) of the POC flux. The faecal pellet flux peaked at 100 m across the shelf, suggesting krill defecating at depth effectively counteracted attenuation in the upper ocean. Our findings emphasise the importance of zooplankton-mediated processes in determining the particle flux and the benefits of resolving the vertical flux at a resolution which incorporates their ecology. It is unclear how changing sea ice dynamics will impact zooplankton, so a process-driven understanding of biogeochemical fluxes is integral for predicting the future of carbon cycling in the Southern Ocean.

1. Introduction

The Southern Ocean is a globally important site of carbon sequestration (DeVries, 2022). This is largely achieved by cool waters with higher carbon dioxide solubility, deep water formation and a strong biological carbon pump (BCP), the process by which organisms mediate the transfer of carbon from surface waters into the deep ocean (Boyd et al., 2024; Volk and Hoffert, 1985). In the Southern Ocean, most total organic carbon is produced as particulates rather than dissolved material (Carlson et al., 2000). These particulates consist of protists, detritus, aggregates and zooplankton faecal pellets, moults and carcasses (Alldredge and Silver, 1988; Turner, 2015; Halfter et al. 2022). The euphotic zone determines the potential upper limit of the biological carbon pump through primary production; however, as these particles sink out of the euphotic zone, they are progressively modified (e.g. by fragmentation or aggregation),

solubilised, remineralised and repackaged. This results in the flux attenuating with depth, often rapidly, as particulate organic carbon (POC) is converted into dissolved inorganic carbon (DIC) and dissolved organic carbon (DOC) (Goldthwait et al., 2005; Martin et al., 1987; Le Moigne, 2019; Volk and Hoffert, 1985). The particle flux can experience intense remineralisation in the upper ocean, releasing dissolved carbon towards the surface and fuelling the microbial loop wherein heterotrophic microbes consume dissolved organic matter and funnel this carbon back to higher trophic levels (Azam et al., 1983). However, ephemeral high production events or zooplankton driven modifications can bypass rapid attenuation near the surface, increasing the proportion of dissolved carbon which is eventually released into deeper waters (Buesseler and Boyd, 2009). High production events may arise after the collapse of a bloom causing rapidly sinking pulse of particulates (Lacour et al., 2023; Manno et al., 2020) and zooplankton can significantly impact the flux through production of faecal pellets and detritivory. Faecal pellet production repackages material into dense, fast sinking particles, contributing to the flux (Cavan et al., 2015; Liszka et al., 2019; Manno et al., 2015). Conversely, detritivory and sloppy feeding can fragment particles, reducing their size and sinking rate, contributing to flux attenuation (Mayor et al., 2014). The balance of these processes is highly dependent upon the resident zooplankton community as well as the composition and bloom stage of the primary producers (Lacour et al., 2023; Le Moigne et al., 2015; Steinberg and Landry, 2017).

Within the Southern Ocean, the Weddell Sea is simultaneously highly productive and a site of deep-water formation, helping to drive the global thermohaline ocean circulation (Tally, 2013). Consequently, it is of global biogeochemical significance. Indeed, the Weddell Sea accounts for ~ 25% of Southern Ocean primary productivity, averaging ~ 477 Tg C a^{-1} (Arrigo et al., 2008). However, this productivity is largely focused on the shelf and the marginal ice zone(Arrigo et al., 2008; El-Sayed and Taguchi, 1981). Iron and light availability typically limit productivity in the Southern Ocean, creating regions of high nutrient availability but low chlorophyll concentration however, sea ice, ice shelf associated melt waters and shelf waters often contain elevated nutrient concentrations due to greater terrigenous inputs and a stronger influence of resuspension, fuelling phytoplankton blooms (Arrigo et al., 2008; Klunder et al., 2014; Middag et al., 2013; Smith and Nelson, 1985). This productivity supports a wealth of secondary consumers, including Antarctic krill (*Euphausia superba*) that directly impact the BCP via the production of dense, fast sinking faecal pellets (FPs), as well as rapid grazing rates exerting top-down pressures on phytoplankton blooms (Schmidt et al., 2018; Whitehouse et al., 2009). Although estimates of krill biomass from the Weddell Sea are scarce as the area is difficult to access due to its remote location and consistent sea ice cover (Atkinson et al., 2017), observed values range from 1-68 g m^{-2} wet weight in open water and 10-100 g m^{-2} under ice (Brierley et al., 2002; Daly and Macaulay, 1988; Guihen et al., 2014). Model based estimates of krill contributions to the BCP suggest the northern Weddell Sea marginal ice zone may be one of the most productive regions in the Southern Ocean, with a potential contribution of up to 325-3350 mg C m^{-2} day^{-1} in spring (Belcher et al., 2019). This high productivity coupled with its hydrography makes the Weddell Sea a site of global biogeochemical importance (Brown et al., 2015; Hoppema, 2004).

As a major contributor to deep water formation, the Weddell Sea generates up to 60% of Antarctic Bottom Water, the most voluminous and densest water mass on earth (Johnson, 2008; Orsi et al., 1999). Carbon sequestration periods can be increased when POC is remineralised in regions where deep water is formed (Baker et al., 2022), and as such these physical processes combined with the intense biological particulate production make carbon sequestration highly efficient in the Weddell Sea (Hoppema, 2004; Nissen et al., 2022; Volk and Hoffert, 1985). The

Weddell Sea is experiencing rapid climate change, with a recent shift towards decreasing sea ice extent and thickness (Joshi et al., 2024). Warming, changes to sea ice and ice shelf melt dynamics have potential to impact both deep water formation and the resident plankton community, which in turn may impact the capacity of the Weddell Sea to act as a carbon sink (Nissen et al., 2022; Zhou et al., 2023). Consequently, improving our understanding of the mechanisms regulating the magnitude of the carbon pump in the Weddell Sea shelf and marginal ice zone, including characterisation of the vertical carbon flux itself, is of vital importance.

This study quantifies and characterises the variability of daily vertical particulate organic carbon and particulate organic nitrogen fluxes across 50, 100 and 150 m in the western Weddell Sea (04/02/2024 – 27/02/2024), using a custom-built drifting sediment trap (DST). The DST was deployed on and off the shelf, within sea ice and in open water. This study aims to characterise the major inputs into the biogeochemical particle flux, and how these change with the environment and across depths. Results provide insight on Southern Ocean carbon cycle drivers by capturing the flux both where the upper limit of carbon flux is determined and the greatest influence on attenuation is exerted (Buesseler et al., 2020).

2. Methods

2.1 Deployment and sampling

The DST was deployed in five occasions from the *RSS Sir David Attenborough* in the Weddell Sea from 04/02/2024 – 01/03/2024 (Cruise number SD035), with each deployment lasting between 11.4 and 22.4 hours (Table 1, Supplementary table 1). The first deployment (S1) took place while sheltering from rough weather, consequently the DST remained tethered to the ship via a line (5 m from the ship) to prevent loss of the trap. Both the trap and the ship drifted ~ 1 km during deployment. Thereafter the trap was deployed freely drifting (where it drifted between 4-13 km Figure 2, Table 1). In the main, the trap was deployed during daylight, with an average of 60% of the deployment taking place between apparent sunrise and sunset (Table 1).

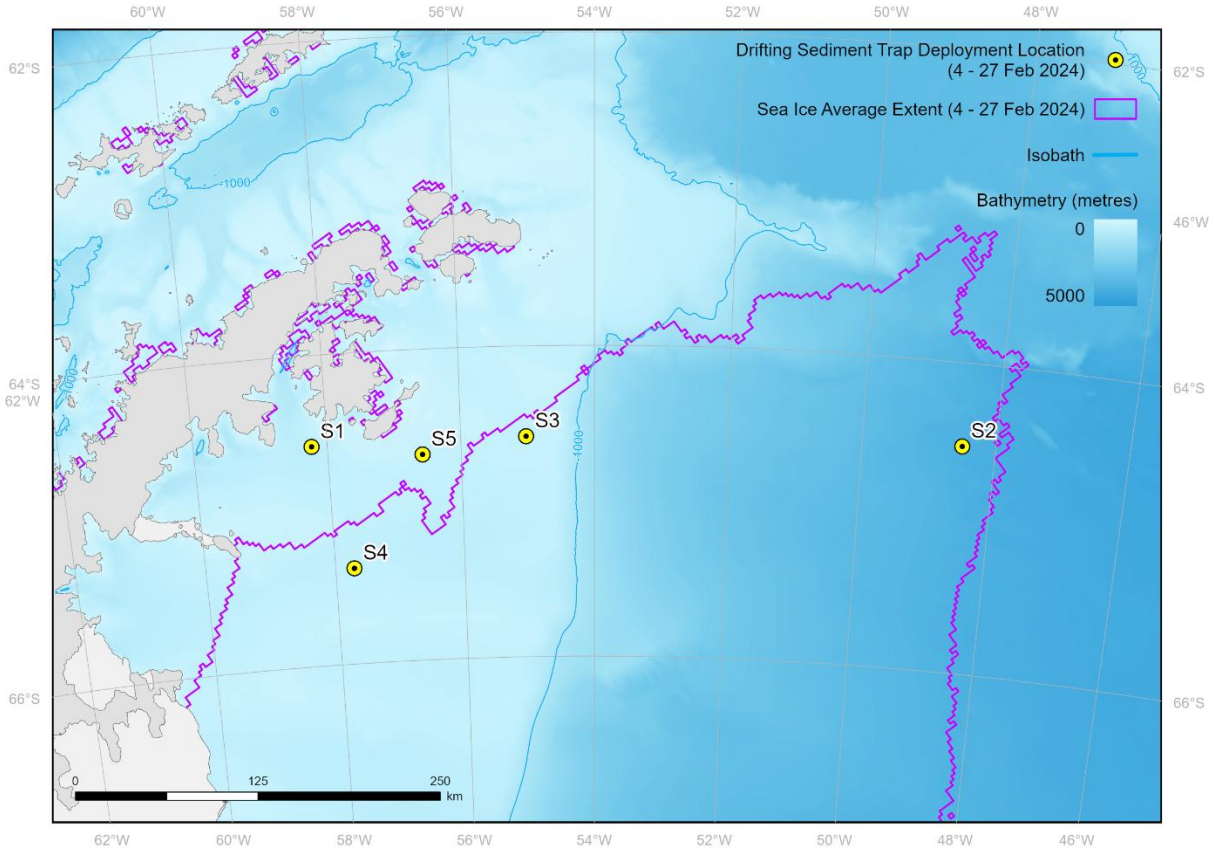

Figure 1. Map of all five deployments across the Weddell Sea during February 2024 with the average sea ice extent (threshold of 15% sea ice concentration) for the entire sampling period in purple. Maps produced by Mapping and Geographic Information Centre, British Antarctic Survey, 2025.

Table 1. Times, daylight duration and distances for each drifting sediment trap deployment. The trap was released in the wester Weddell Sea during February 2024.

Sampling Station	Date and Time deployed (UTC)	Date and Time recovered (UTC)	Deployment duration (decimal hours)	Time the deployment was between apparent sunrise and sunset (daylight hours) (%)	Distance Trap drifted (m)
S1	04/02/2024 12:28:00	04/02/2024 23:52:00	11.4	40	931
S2	07/02/2024 23:00:00	08/02/2024 17:03:00	18.1	92	5305
S3	16/02/2024 11:54:00	17/02/2024 00:11:00	22.4	38	3826
S4	27/02/2024 01:02:00	27/02/2024 21:34:00	12.1	72	6419
S5	29/02/2024 14:05:00	01/03/2024 12:31:00	20.5	58	13479

The custom DST (developed in house at the British Antarctic Survey) consists of a surface float fitted with an Iridium beacon, a vertical array of carousels (at 50, 100 and 150 m depth) with collection cannisters and a 10 kg weight at the bottom of the line. The three carousels are each fitted with four steel, poison-free 6.2L collection canisters with an opening of 0.012 m^2. The DST is fitted with a messenger fired closing mechanism. At the end of the deployment, the messenger was released prior to recovery, closing the lids on the collection cannisters and preventing contamination which could result in an overestimation of the flux as the trap is hauled onboard. With each deployment a Conductivity-Temperature-Depth (CTD) profile was taken (Richter et al., 2026), equipped with the following instruments: a Sea-Bird SBE 9plus CTD system which included two Sea-Bird SBE3plus temperature sensors, Sea-Bird SBE4C conductivity sensors and a Paroscientific Digiquartz pressure sensor, a WETLabs Coloured Dissolved Organic Matter fluorometer and a SBE18 pH sensor (which replaced CDOM fluorometer from S3). Due to logistics, the closest CTD profile (-65.4087 N, -57.8138 E) to S4 (-65.3866 N, -57.7157 E) was 5.16 km away. The mixed layer depth (MLD) was identified by ascertaining the depth at which the density was equal to the density at 10 m + 0.03 kg m^3 following (de Boyer Montégut et al., 2004). Analysis and figure generation of CTD profile data was carried out in R (version 4.3.2).

To calibrate the CTD fluorometer, chlorophyll-a concentrations were sampled onboard using size-fractionated method, following Robinson et al., (2002). In short, 100 ml of sea water was filtered onto 20 µm, 2 µm, and 0.1 µm polycarbonate filters. These filters were placed into 15 mL falcon tubes, and frozen at -80°C until analysis. For analysis, 10 ml of acetone was added to the filter for up to 24 hours and stored at -20°C. Samples were then left to equilibrate to room temperature under dark conditions prior to measuring their raw fluorescence value using a fluorometer (Turner Designs Instrument, Model no. 7200-000). These results were processed against a standard calibration to gain the chlorophyll-a concentration in µg L^{-1} (Wilkinson, 2026). Following analysis using Pearsons's correlation ($R^2 = 0.8022$, $p < 0.001$, $n = 121$), a conversion of 3.1823 x - 0.0700 was applied to the CTD fluorometry measurements (where x is equal to the CTD fluorescence).

2.2 On-ship sample preparation

Once recovered, the DST was processed immediately. Water was decanted from the DST carousel into 10L carboys (pre-rinsed three times with Milli-Q). The carousels were rinsed three times with Milli-Q water to ensure all particulates entered the carboys. Throughout, each carboy was gently but thoroughly stirred immediately prior to any subsampling to ensure representativeness. As the trap was poison free, no pre-filtering for 'swimmers' (dead zooplankton which had actively entered poisoned traps) was necessary. For particulate organic carbon (POC), particulate organic nitrogen (PON), 600 ml of water was filtered onto pre-combusted (450°C, 16 hrs), pre-weighed glass fibre filters (GF/F, 25 mm, 0.45 µm pore size, Whatmann) and rinsed with Milli-Q water (under < 20 mbar of vacuum pressure). Blanks (n = 5) were created by filtering 600 ml of Milli-Q water onto pre-combusted glass fibre filters as above. With the exception of S1 (where no replicates were taken), two replicates were taken from each depth and each deployment. All particulate samples were then air-dried for 24 hours in a fume hood and stored at -20°C until analysis at British Antarctic Survey, Cambridge, UK. To characterise the particles within the flux (e.g. faecal pellets, eggs), two 250 ml subsamples were taken per depth and deployment. These quantitative samples were then spiked with 13 ml of 37 % formaldehyde to reach a final concentration of 2% formalin.

2.3 Elemental analyses

POC, PON and blank samples were fumed for 24 hours with 37 % HCl in a desiccator to remove the inorganic carbon content. POC and PON filters and filter blanks were placed in sterile nickel capsules, and analysed using a CE Instruments NA2500 elemental analyser, calibrated using an acetanilide calibration standard with a known % C and % N of 71.09 % and 10.36 % respectively. Standards were interspersed regularly between samples to measure and correct for drift with an analytical precision of ±0.3 %. Flux (mg m^{-2} day^{-1}) was calculated using the following equation (Eq. 1).

$$(Eq.\,1) \qquad Flux\ (mg\ m^{-2} day^{-1}) = \frac{m}{A * d}$$

Where *m* is the mass of the particulate element (corrected using average of all blanks) to the total cannister volume (6.2 L), *A* is the area of the cannister opening (0.012 m^2) and *d* is the duration (days) the trap was drifting (our observations were normalised to per day). POC and PON samples were then corrected using blanks. Analysis and figure generation and any statistical analysis of all fluxes and their characterisation (e.g. faecal pellets and egg abundance) were carried out in R (version 4.3.2).

2.4 Faecal pellet and egg abundance and size

Faecal pellet (FP) samples were left to settle in the lab for > 48 hours. 200 ml of supernatant was carefully decanted off using a syringe. The remaining 50 ml was analysed under an Olympus SZX16 dissecting light microscope. Images of each sample were taken using a Canon EOS 60D DSLR camera, with size measurements subsequently analysed using ImageJ (Version 1.54g). FP were classified into three shapes, cylindrical, round (i.e. an almost sphere shape) and oval, with volume calculated using geometrical equations for a cylinder, sphere and oval respectively. FP abundance and total volume were normalised to total cannister volume and flux was calculated using Eq. 1. To estimate carbon content in cylindrical faecal pellets a conversion factor, derived from Antarctic cylindrical faecal pellets (Krill), of 0.08 mg C mm^{-3} was used (Pauli et al., 2021).

Krill eggs were identified by size (~ 670 µm, George and Stromberg, 1985), with flux calculated and size estimated using the same method as faecal pellets. To estimate krill egg carbon, a conversion factor of 17.175 µg C per egg was calculated from Ikeda (1985) by averaging the carbon content (of embryos stage I-IV) and an average hatching success of 68.4% was applied, as only eggs which do not hatch contribute to the POC flux (Harrington and Ikeda, 1986). No zooplankton moults were observed in any of the samples analysed by microscopy.

2.5 Microplankton community abundance

A detailed description of collection and analysis methods are available in the supplementary (Supplementary methods). In brief, microplankton (defined here as 20-100 µm) samples were collected from the euphotic zone using a CTD and Niskin bottles and preserved with 5 mL acid Lugols' solution at 4 °C until analysis at Plymouth Marine Laboratory, Plymouth, UK. Samples were then concentrated through settling, and imaged using a FlowCam IV (Yokogawa Fluid Imaging Technologies) fitted with a x10 objective and 100 µm flow cell. Subsequent images were processed using VisualSpreadsheet (v4.19.3), with particles classified to genus where possible (otherwise particles were assigned to broader taxonomic groups e.g. dinoflagellate, ciliate etc). Ice associated phytoplankton taxa (commonly *Fragilariopsis* spp., *Entomoneis* spp., *Nitzschia* spp., *Cylindrotheca* spp. and large single centric diatoms) were subsequently compared with total protist abundance to evaluate their contribution to community structure.

2.6 Satellite imagery

Average sea ice extent was calculated as a median of daily sea ice concentration layers from the 4th to the 27th of February 2024, assuming threshold for an ice-covered pixel is 15% of its area using Advanced Microwave Scanning Radiometer-EOS 89-GHz channels (AMSR-E) (Spreen et al., 2008). Sea ice concentration data for individual sampling stations was generated as above selecting the values for the pixel corresponding to the geographic location of the sampling station, with pixel sizes ranging between 20-43 m. Bathymetry was compiled from the GEBCO bathymetric compilation group (GEBCO Bathymetric Compilation Group, 2025) with maps generated in ArcGIS Pro (version 3.6.0). Satellite images, including Sentinel-1 to 3 and Landsat-8 and 9, were downloaded from Google Earth Engine, taking into account the DST track geographical extent and deployment time. For the maps above the closest to the deployment time images were used. Subsequent images were prepared in QGIS (version 3.44).

2.7 Statistics

Spearman's rank correlation was used to compare the POC flux against hydrological conditions as measured by the most proximal CTD profile. Hydrological conditions were represented by maxima and minima within the profile (for example chlorophyll maximum, temperature maximum, salinity minimum) (Supplementary table 2). Kruskal Wallace tests were used to determine if individual cylindrical faecal pellet volume changed across sampling depths (50, 100 and 150 m) across each of the five drifting sediment trap deployments. All statistics were carried out in R (Version 4. 3. 2).

3. Results

3.1 Hydrological context

The DST was deployed in and amongst sea ice at stations S3 and S4 (Figure 2C, D). Though the rest of the stations have been classed as 'ice free', a substantial number of icebergs were present at S1 and S5, with S5 (Figure 2A, B, E) having been ice covered the previous day and S2 having been ice-covered two days prior (Supplementary table 1, Supplementary figure 2, 3).

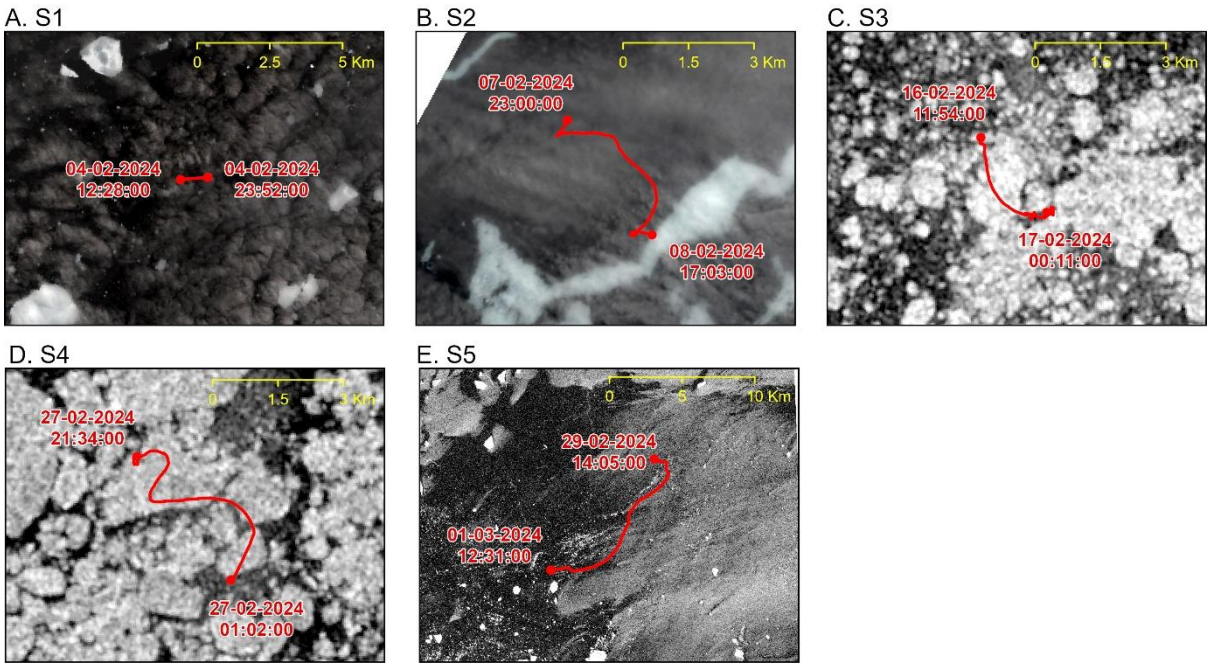

Figure 2 A-E. Satellite imagery with overlayed track data for the drifting sediment trap (Weddell Sea, February 2024). At S1 (A.) the drifting sediment trap was deployed next to the ship. Images produced by Mapping and Geographic Information Centre, British Antarctic Survey, 2025. All times are recorded in coordinated universal time (UTC).

Temperature and salinity profiles of the top 150m of each station revealed the MLD ranged from 11-36 m (Figure 3, Supplementary table 1). Consequently, all flux measurements were taken below the MLD. S1 was the most productive station, with a chlorophyll peak of 2.73 µg L^{-1} at 8 m. In contrast S2 was the least productive station, with a chlorophyll maximum of 0.60 µg L^{-1} recorded at a considerable depth (89 m). The two 'ice stations', S3 and S4 had very low temperatures at the surface (-1.60 to -1.45 °C) and at depth (> 100 m, -1.77 to -1.59 °C). S4 had a warmer intrusion (maximum of -1.13 °C) at 16-34 m. All stations had fresher water at the surface, however this fresher layer was deepest at S2 and the two ice stations, S3 and S4.

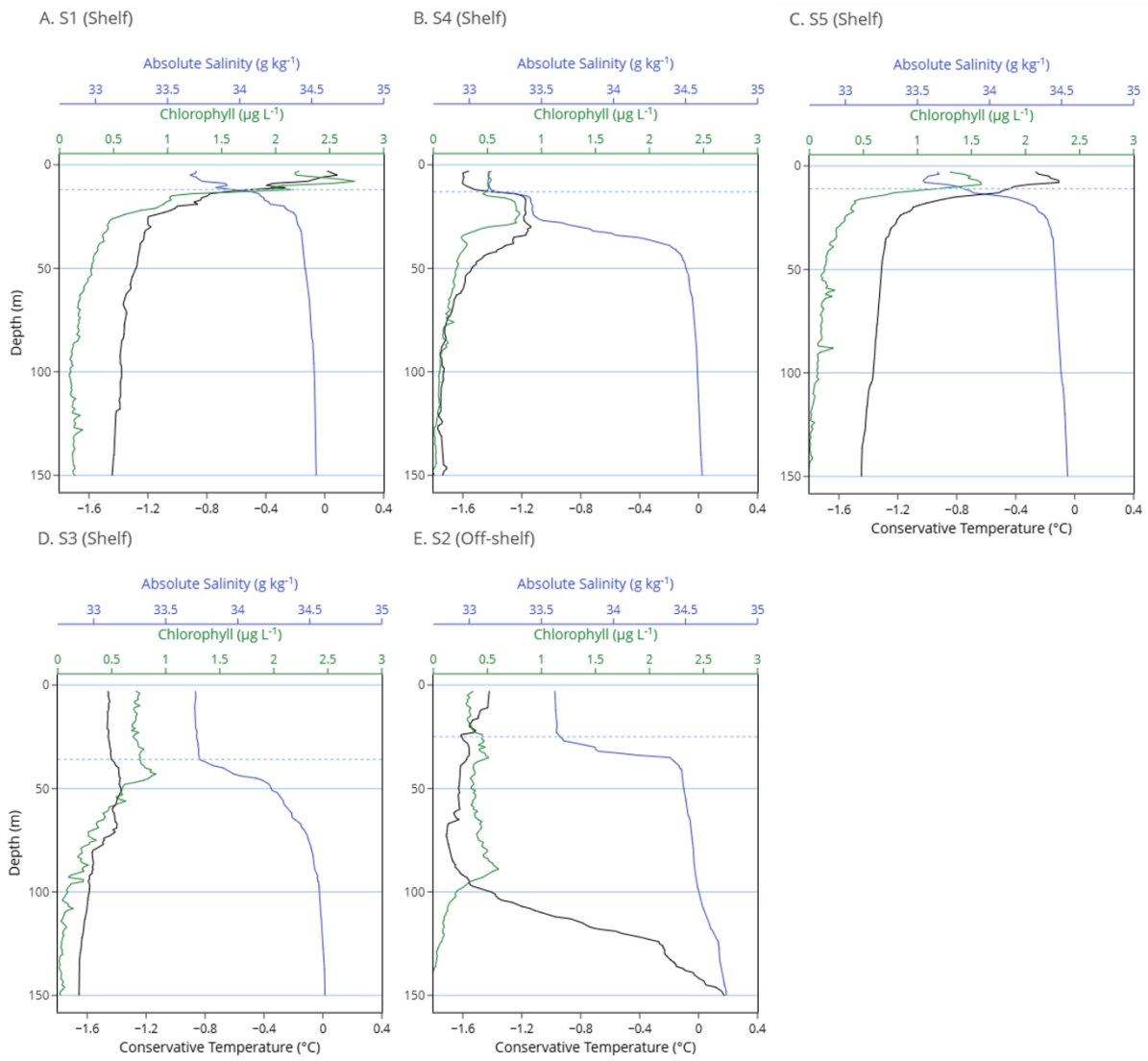

Figure 3. A-E, Conservative Temperature (°C), Absolute salinity (g kg^{-1}) and Chlorophyll (µg L^{-1}) of the upper 150 m across the stations of the floating trap deployment (Weddell Sea, February 2024). The mixed layer depth is indicated by the dotted line, with solid lines indicating the collection depths for the drifting sediment trap. Profiles were taken at deployment location with

the exception of S4, which was the closest profile, taken 5 km from the deployment location (due to the presence of ice).

3.2 The Particulate Flux: Biogeochemical Composition

The highest POC fluxes were observed at S1, wherein the POC flux increased with depth reaching a maximum of 364.1 mg C m^{-2} day^{-1} at 150 m depth (Figure 4 A). Higher POC fluxes were also observed at S3, however with an opposing trend, with a maximum of 220.0 mg C m^{-2} day^{-1} at 50 m, decreasing to 106.0 mg C m^{-2} day^{-1} at 150 m. S2, S4 and S5 had relatively uniform POC fluxes throughout all depths, with S5 showing a small increase at 100 m. S2 is the station with the lowest POC flux, averaging 51.3 mg C m^{-2} day^{-1} across all depths. Patterns in PON fluxes largely mirror the POC, with the highest PON fluxes at S1, and the lowest, and most uniform PON flux across all depths at S2 and S4 (Figure 4 B).

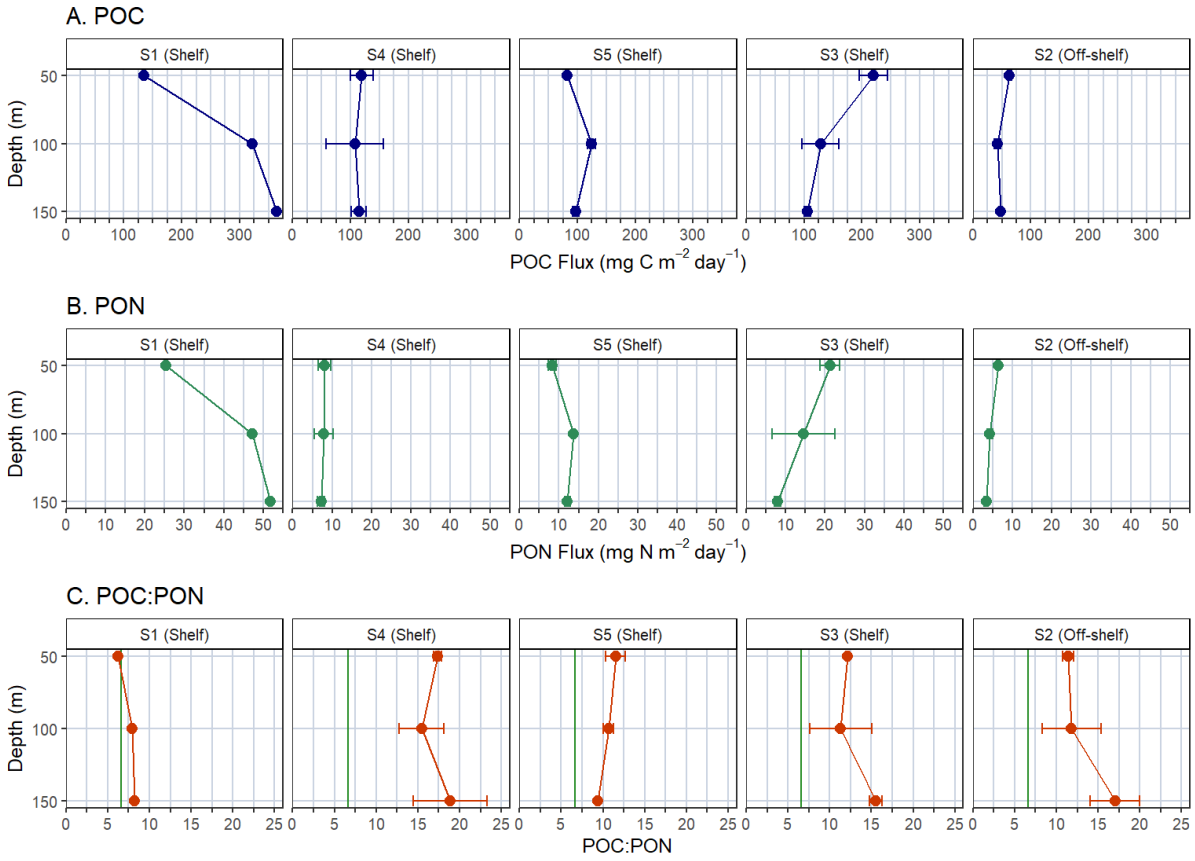

Figure 4. Mean vertical particulate flux (± standard deviation) observed at 50, 100, and 150 m across five deployments in the Weddell Sea (February 2024). A. particulate organic carbon flux, B. particulate organic nitrogen flux, C. POC:PON of the particle flux (atomic, ± standard deviation), with green line indicating the Redfield ratio of C:N (6.63). Stations are numbered by sampling order, but the panel is arranged in a gradient from on shelf to off-shelf (left to right).

The POC:PON atomic ratios of sinking material tended to be substantially higher than Redfield (C:N, 6.63) (Redfield, 1934), with a median of 11.51 across all stations and depths. S1 had a POC:PON ratio closest to the Redfield ratio, followed by the S5 (Figure 5). S5 became more similar to Redfield at depth whereas S1 deviates from Redfield at the surface. The remaining

stations (S2, S3, and S4) all had the largest POC:PON ratios at 150 m depth, with S4 having the highest average POC:PON ratio observed of 14.76.

POC flux was compared against multiple CTD parameters (Supplementary table 2). Of the parameters tested, POC flux and the chlorophyll maximum were positively correlated (Rho =0.71, d.f. = 13, p value = 0.003, Supplementary figure 1A) and POC flux and the depth of the chlorophyll max negatively correlated (Rho = -0.64, d.f. = 13, p value = 0.009, Supplementary figure 1B) and finally POC flux and the salinity maximum were negatively correlated (Rho = -0.71, d.f. = 13, p value = 0.003, Supplementary figure 1C), though it should be noted that no significant correlation was present with the salinity minimum.

3.3 The Particulate Flux: Faecal pellets and eggs.

Across all stations and depths, the FP flux contributed a median of 47.9 % of the carbon flux (Figure 5 A). The faecal pellet flux was strongly driven by krill defecation, since cylindrical faecal pellets (FP) made up the majority of pellets, representing 98% of the total FP volume flux (when summed across all stations and depths) (Supplementary figure 4). Round and oval pellets had a minimal presence in the traps (each representing 1% of total faecal pellet volume). Depth resolved patterns of FP contributions to the carbon flux did not mirror those of POC flux (Figure 4 A). However, stations with a higher POC flux generally had a greater FP flux (e.g. S1) and S2, with the lowest POC flux also has the lowest FP flux. S5 had the highest percentage of carbon represented by cylindrical FP, with a maximum of 99.0% at 150 m (Supplementary table 3). On the other hand, S2 and S4 had the lowest percentage carbon represented by FP, with both stations having minima at 50 m (S2, 17.4 % and S4, 25.8 %). Within each station, patterns in individual cylindrical FP volume (Figure 5 B.) were generally uniform across depth, with the exception of S1 and S5, where the individual cylindrical FP volume increased with depth (chi square = 27.21, $p < 0.001$, df = 2 and chi square = 14.35, $p < 0.001$, df = 2 respectively, supplementary table 4).

Krill eggs were present in the particulate flux at S1 and S3 (and absent from all other stations). S1 had the highest krill egg flux of 3990 eggs m^2 day^{-1} at 100 m and lowest krill egg flux of 1958 eggs m^2 day^{-1} at 150 m (Supplementary table 5). These eggs were estimated to represent between 2.9 – 6.7 % of total POC at their respective stations (Figure 6). S3 also had krill eggs present, estimated to represent 5.1 % of the total POC flux.

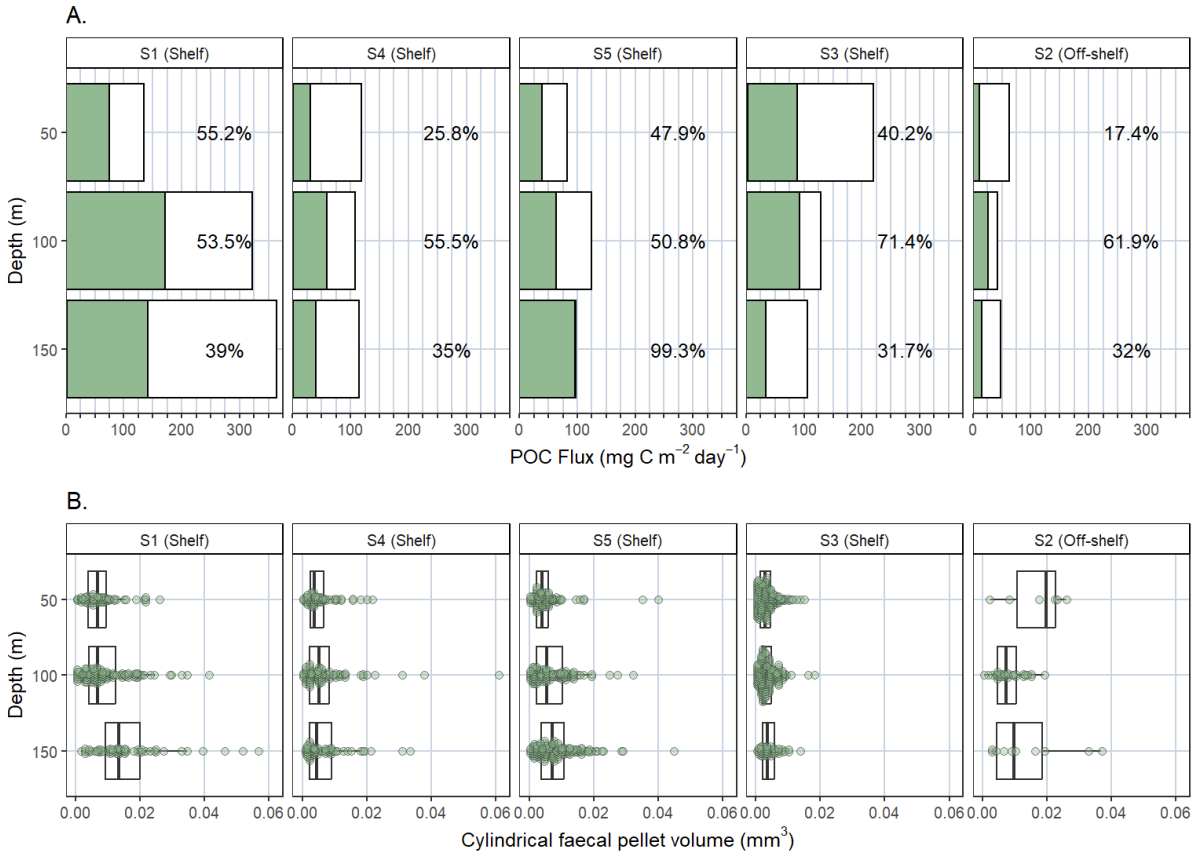

315

316 Figure 5 A. Estimated carbon content of all faecal pellets (green) as a proportion of the total
317 POC flux (white) at each station. The estimated percentages of the total POC represented by
318 faecal pellets are presented adjacent to each bar. B. Individual particle volumes of each
319 cylindrical faecal pellet identified. Throughout, stations are numbered by sampling order, but
320 the panel is arranged in a gradient from on shelf to off-shelf (left to right) in the Wedell Sea
321 (February 2024).

322

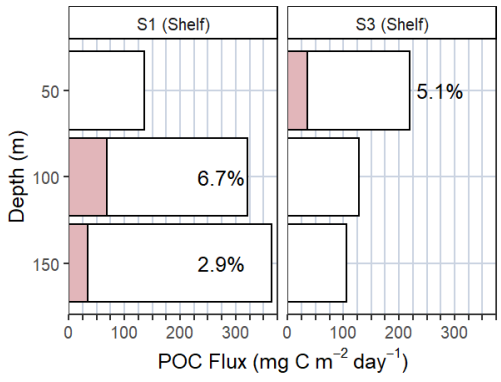

323

324 Figure 6. Estimated carbon content of Krill eggs (pink) compared with the mean total POC flux
325 (white) in the Weddell Sea (February 2024) at stations where krill eggs were present. The
326 estimated percentages of the total POC represented by krill eggs are presented adjacent to
327 each bar

4. Discussion

The POC flux that we measured in the western Weddell Sea varied from 42.5 - 364.1mg C m^{-2} day^{-1} (mean of 123.2 mg C m^{-2} day^{-1}), with higher fluxes observed on the shelf (S1, S4, S3, S5) than off the shelf (S2), correlating with the magnitude and depth of the chlorophyll maximum (Figure 4, Supplementary figure 1A and B). Despite the importance of the Weddell Sea in global biogeochemical cycling and climate change disrupting sea ice production, contemporary direct particulate flux measurements in the Weddell Sea remain scarce (Joshi et al., 2024). Globally, 75% of POC fluxes at 150 m are ≤ 90 mg C m^{-2} d^{-1}, indicating the majority of our stations were well above this metric (Mouw et al., 2016). Previous studies in the northern and eastern Weddell Sea have reported POC fluxes ranging from 24 to 112 mg C m^{-2} day^{-1} at depths of 150–250 m, with occasional extreme values exceeding 1000 mg C m^{-2} day^{-1} during spring bloom conditions (von Bodungen, 1986; Cadée, 1992; Dunbar, 1984; Isla et al., 2006; Wefer et al., 1990). The fluxes observed in our study fall well within this broad range, although the absence of extreme values likely reflects sampling late in the productive season (end of February), as the high values (> 1000 mg C m^{-2} day^{-1}) reported by Cadée (1992) and von Bodungen et al., (1986) both occurred in spring (November/December). There are only a few observations of PON fluxes within the Weddell Sea. Previous studies reported PON fluxes ranging from 0.51 -20.86 mg N m^{-2} day^{-1} (10-230 m) (Thomas et al., 2001; Michels et al., 2008) which is the same order of magnitude as our observations (3.4 - 51.9 mg N m^{-2} day^{-1}).

In order to prevent the trap drifting into rough weather, the trap was tethered to the ship on its first deployment at S1, the station closest to the coast. Tethered traps have the potential to behave differently from free drifting traps, with lateral advection across the trap potentially reducing the collection efficiency of the trap (Buesseler et al., 2000). To help mitigate the impact of tethering, the ship was allowed to drift alongside this trap where reasonably possible, however collection efficiency may still have been impacted. Despite tethering, patterns in the magnitude and characterisation of the flux present at S1 appear to well reflect the productive conditions present at this site. Station S1 also had the highest chlorophyll concentration observed (2.73 µg L^{-1}, Figure 3), the highest POC and PON fluxes (Figure 4) and a mean POC:PON ratio of 7.45; close to the Redfield ratio of phytoplankton (6.63, Redfield, 1934). Together these values suggest high productivity and export with relatively fresh particulate material which had experienced little nitrogen remineralisation (Copin-Montegut and Copin-Montegut, 1983; Wakeham et al., 1997) (Figure 5). Indeed, the chlorophyll maximum at S1 is in line with bloom-like conditions observed within the wider Weddell Sea (von Berg et al., 2020), however in this particular region of the shelf, chlorophyll concentrations > 5 µg L^{-1} have been observed (Salyuk et al., 2025). This suggests S1 was productive, but the bloom was not as strong as is possible on the shelf, perhaps a result of sampling towards the end of the productive season. The higher POC fluxes observed consistently across the shelf (S1, S3, S4, S5) likely reflects the higher concentrations of (micro)nutrients (such as iron and manganese) compared to the Weddell Sea open waters (Balaguer et al., 2023; Klunder et al., 2014; Middag et al., 2013). Moreover, the shallower water column of the shelf stations supports mixing and resuspension that facilitates nutrient resupply to the surface (Isla et al., 2006; Pudsey and King, 1997; Semper and Darelius, 2017).

Although the sea ice edge can also promote productivity, there were no strong patterns observed in the particulate flux between sea ice and ice-free stations (Arrigo et al., 2008; Lannuzel et al., 2016; Smith and Nelson, 1985). This likely reflects the highly dynamic nature of

sea ice during the sampling period. Stations were classified as ice-free based on conditions present during deployment, however, as the ice was constantly shifting, we suggest that the particulate flux integrated longer-term patterns in sea ice coverage which were minimised when we only accounted for deployment conditions. For instance, according to satellite images and coverage data, S2 (classed as 'ice free') was ice-covered two days prior to sampling (Supplementary figure 2, 3), and S5 had a variable sea ice coverage throughout February and January (Supplementary figure 5). The likelihood that most of our stations are heavily influenced by sea ice is supported also by patterns in POC:PON. With the exception of S1, the POC:PON ratio of the flux varies from 9.35 -18.84. These ratios exceed both classic Redfield ratio for phytoplankton (6.63, Redfield, 1934) as well as the Southern Ocean specific ratio (mean of 6) (Tanioka et al., 2022). Sinking particulate material commonly has a higher C:N relative to fresh phytoplankton, as nitrogen is preferentially absorbed by grazers and microbes with depth (Atkinson et al., 2012; Copin-Montegut and Copin-Montegut, 1983; Wakeham et al., 1997). For example, fresh Krill FP C:N has been shown to range between 3.2-13.2 (Atkinson et al., 2012; Manno et al., 2024). However, our range of ratios exceed values stated above, suggesting the potential for an additional influence of ice associated biota across the stations. Ice associated microplankton often have elevated and more variable C:N ratios as compared to pelagic phytoplankton, with ice associated microplankton C:N ranging from 6.2- 12.6 (Cozzi and Cantoni, 2011; Kennedy et al., 2002; Niemi and Michel, 2015) and pelagic Southern Ocean phytoplankton broadly ranging between ~ 6-8 (Arrigo et al., 1999; Hoppe et al., 2017). Indeed, microplankton community data from stations S2-S5 indicate that ice associated microplankton comprise and average 11.5-26.4% (mean of 18.2 %) of protists up to the 1% photosynthetically available radiance depth (Supplementary table 6). In addition, the mean contribution of ice associated microplankton at S1 is lower (7.7%), reflecting POC:PON patterns in our data. These findings highlight the limitations of categorising flux observations solely based on instantaneous ice conditions in dynamic polar environments.

Antarctic krill exerted a dominant control on the particulate carbon flux across shelf stations. Cylindrical FP, reliably identifiable as krill-derived, accounted for 98 % of total FP volume (with round and oval pellets accounting for ~ 1% of total FP volume each). 88 % of cylindrical FP were wider or equal to 80 µm, indicating that they likely originated from *E. superba* (Atkinson et al., 2012). The dominance of different FP types can be highly variable, dependent upon food availability and the zooplankton community composition (Manno et al., 2015; Perhirin et al., 2025). However, in regions where krill dominate, krill FP have been found to represent > 80% of all sinking particles (Cavan et al., 2017), in good alignment with our data. Our traps were deployed between 11.4 and 22.4 hours, and shorter deployments may favour faster sinking larger pellet sizes such as krill FPs (Baker et al., 2020; Perhirin et al., 2025). However, our results are also in good agreement with longer-term moored sediment traps within the Weddell Sea, where pulses of krill FP flux dominate the particulate flux on the shelf (Bathmann et al., 1991; von Bodungen, 1986; Dunbar, 1984).

Using a conversion factor of 0.08 mg C mm^3 (Pauli et al., 2021), cylindrical FP contributed between 17.4 and 99.0% of carbon to the total POC flux (with a median of 47.9 %), with the remaining carbon attributed to detritus (largely phytodetritus) (Figure 5 A). The carbon content of krill FP is not fixed, varying with grazing rates and food availability (Atkinson et al., 2012). Indeed, Pauli et al., (2021) reported a standard deviation of ±0.044 C mg mm^3 (equivalent to ± 55%), which could extend our estimated range of FP contribution to the POC flux, with the median value ranging between 26.3-74.2%. Despite this variability, stations with higher POC fluxes generally exhibited higher faecal pellet fluxes, indicating a strong coupling between krill

activity and flux magnitude. These observations reinforce previous findings that krill-mediated repackaging of organic matter into large, dense, fast-sinking particles is a key pathway for carbon export in the Southern Ocean (Belcher et al., 2017, 2019; Cavan et al., 2019; Manno et al., 2022; Trinh et al., 2023).

POC fluxes increased or remained relatively stable with depth across most stations (S1, S2, S4, S5) rather than attenuating rapidly. The absence of attenuation in our data may be explained by pulses of productivity in the recent past, lateral advection of material, zooplankton producing particulates at depth and or a lack of zooplankton grazing on/fragmenting particles (e.g. Cavan et al., 2015; Freudenthal et al., 2001; Le Moigne et al., 2015; Smith et al., 2018). While temporal mismatches between production and collection cannot be fully excluded, physical processes such as lateral advection should have a minimal impact on 'catch efficiency' given the sediment trap was free drifting for stations S2-S5 (Buesseler et al., 2000).We suggest instead that the consistent vertical patterns in faecal pellet flux are strongly indicative of zooplankton mediated control. Across most stations (S1-S4), krill faecal pellet flux peaked at 100 m, irrespective of surface chlorophyll concentration and environment. We propose this result is indicative of krill vertical migration or movement, and production of pellets at depths between 50 and 100 m (below the MLD). Patterns in krill vertical distribution are both highly variable and seasonal, although in summer krill often migrate to depths of ~ 100 m during diel vertical migration, krill are strong swimmers and can also disperse throughout the water column, even migrating to the seabed (Bahlburg et al., 2023; Clarke and Tyler, 2008; Schmidt et al., 2011; Smith et al., 2025; Tarling et al., 2018). Vertical movements of krill (i.e. krill spending time at depths of 50 - 100 m) well reflect the trends in our data. In addition, individual FP volumes remained largely consistent with depth across stations (Figure 5 B), suggesting that relatively little FP fragmentation took place between 50 and 150 m. As discussed above, this may support the hypothesis that krill are defecating at depth, meaning less opportunity for FP to fragment before they are collected at 100 or 150 m. Consistent FP volumes with depth may also reflect rapid sinking speeds as well as low fragmentation rates (either from higher particle integrity or minimal interaction with detritivores) (Atkinson et al., 2012; Briggs et al., 2020; Mayor et al., 2014). Indeed, at S1 and S5, cylindrical faecal pellet volumes significantly increase with depth, and have a lower POC:PON ratio which is relatively consistent with depth, likely indicating a pulse of relatively fresh material is caught in the trap, with rapid sinking of larger pellets. However, given that krill faecal pellet flux peaks at 100 m across stations S1-S4 (regardless of whether patterns in the POC:PON ratio indicate a recent 'pulse' of material or otherwise) we suggest a behavioural component (i.e. vertical migration or movement) is also exerting a significant influence on patterns in particulate fluxes and that overall, krill FP have potential to strongly impact export as well as upper ocean fluxes.

By producing faecal pellets below the mixed layer rather than at the surface, migrating krill effectively bypass near-surface remineralisation, enhancing the efficiency of carbon export (Liszka et al., 2019; Steinberg and Landry, 2017). Given estimated sinking rates of krill pellets (27–1218 m day^{-1}, mean of 309 m day^{-1}; Atkinson et al. 2012) a substantial fraction of this material could reach the seafloor on the shelf (average depth of 421m) within <1-15 days, contributing directly to benthic carbon supply and enhancing long-term sequestration. Carbon-specific krill pellet degradation rates have been estimated as a 23-30% loss at 300 m and up to a 35% loss at 500 m (Pauli et al., 2021). Consequently, across the shelf stations (S1, S3, S4, S5), between 19.8-111.2 mg C m^2 day^{-2} could reach the seafloor. The contribution of krill to the particulate carbon flux was not limited to FPs. Krill eggs present at stations S1 and S3 potentially contributed (2.9-6.7 %) to the POC flux (Figure 6). The available food environment

has a significant impact on maternal condition, egg quality and therefore hatching success (Quetin and Ross, 2001; Steinke et al., 2024; Yoshida et al., 2011). A substantial but undetermined fraction of these eggs will lead to deep carbon export, either through failure to hatch or through hatching to larvae which are non-viable or eaten while still at depth (Perry et al., 2020). Overall, our results highlight that krill eggs have the potential to contribute significantly to the particulate carbon flux, although their contribution is yet unquantified at an ocean scale.

5. Conclusions

This study provided observations of the particulate flux in the upper western Weddell Sea across multiple depths, a region of global importance for carbon sequestration and deep-water formation. We demonstrated that particulate fluxes in the upper 150 m are strongly structured by shelf processes, ice-associated production and zooplankton activity. POC and PON fluxes were higher on the shelf than open ocean, reflecting enhanced nutrient supply and biological productivity in shelf waters. In contrast, no clear distinction was found between sea ice and ice-free stations, reflecting the constant movement of the ice and that often our 'ice free' sites were still influenced by ice.

Krill exerted a strong control on the carbon flux across all shelf sites, with over 98 % of all FP belonging to krill, and contributions of up to 99 % of the POC flux emphasising the role of zooplankton repackaging in mediating carbon export. The peak in FP flux occurred consistently at 100 m across the shelf, suggesting krill are producing FPs at depth. Krill eggs are a poorly constrained component of the flux but our results highlight their potential role as a significant pathway for carbon transfer, particularly towards the end of the productive season where they may contribute up to 7 % of POC flux.

As climate change influences sea ice dynamics, the Southern Ocean is subject to dramatic change, and it is unclear how zooplankton communities may react. Our findings show the importance of zooplankton mediated processes in driving carbon export within the upper 150 m, a region where particulate modification is most intense. Consequently, it is vital that biogeochemical studies in the euphotic zone, incorporate zooplankton processes (particularly vertical migration or movements) to obtain a representative, process-based understanding of carbon cycling in a rapidly changing Southern Ocean.

Author contributions

FA prepared the original manuscript with contributions (review and editing) from all co-authors. FA collected data alongside ER, SF and KS, and conducted analysis with guidance from CM, CM contributed to conceptualisation of the project and equipment used with GF designing and building the custom equipment. EF analysed phytoplankton data and provided guidance on their interpretation. MR processed and quality checked the CTD data, BW collected chlorophyll concentration data for the calibration of the fluorescence sensor. CM, AA, KS and SF contributed to funding acquisition.

Competing Interests

The authors declare that they have no conflict of interest

Financial support

This work was completed as part of the Processes Influencing Carbon Cycling: Observations of the Lower limb of the Antarctic Overturning (*PICCOLO*) project [NE/P021352/1, NE/P021409/1 and NE/P021395/1]. AA's contribution was also funded by the Worldwide Fund for Nature.

Data availability

POC, PON and faecal pellet data are available from the British Oceanographic data centre under the following DOIs 4A9FFBA99AB8E9BAE0637086ABC07E96, 4AA0669048E30212E0637086ABC0AF43, data for the chlorophyll calibration are available from the British Oceanographic data centre under 10.5285/4f7aed48-816a-d8cf-e063-7086abc055b4. CTD data held on Zenodo, under 10.5281/zenodo.20849254. Sea ice concentration data using the AMSR-2 satellite are publicly available here https://data.seaice.uni-bremen.de/modis_amsr2/, thanks to Spreen et al., (2008)

Acknowledgements

We thank everyone associated with cruise SD035 on the RRS Sir David Attenborough. We thank the reviewers for their helpful comments. We thank the MAGIC team at British Antarctic survey, in particular Tom Hughes and Aliaksandra Skachkova for their assistance with mapping and geospatial data.

References

Alldredge, A. L. and Silver, M. W.: Characteristics, dynamics and significance of marine snow, Prog. Oceanogr., 20, 41–82, https://doi.org/10.1016/0079-6611(88)90053-5, 1988.

Arrigo, K. R., Robinson, D. H., Worthen, D. L., Dunbar, R. B., DiTullio, G. R., VanWoert, M., and Lizotte, M. P.: Phytoplankton Community Structure and the Drawdown of Nutrients and CO_2 in the Southern Ocean, Science (1979)., 283, 365–367, https://doi.org/10.1126/science.283.5400.365, 1999.

Arrigo, K. R., van Dijken, G. L., and Bushinsky, S.: Primary production in the Southern Ocean, 1997–2006, J. Geophys. Res. Oceans, 113, https://doi.org/10.1029/2007JC004551, 2008.

Atkinson, A., Schmidt, K., Fielding, S., Kawaguchi, S., and Geissler, P. A.: Variable food absorption by Antarctic krill: Relationships between diet, egestion rate and the composition and sinking rates of their fecal pellets, Deep Sea Research Part II: Topical Studies in Oceanography, 59–60, 147–158, https://doi.org/10.1016/j.dsr2.2011.06.008, 2012.

Atkinson, A., Hill, S. L., Pakhomov, E. A., Siegel, V., Anadon, R., Chiba, S., Daly, K. L., Downie, R., Fielding, S., Fretwell, P., Gerrish, L., Hosie, G. W., Jessopp, M. J., Kawaguchi, S., Krafft, B. A., Loeb, V., Nishikawa, J., Peat, H. J., Reiss, C. S., Ross, R. M., Quetin, L. B., Schmidt, K., Steinberg, D. K., Subramaniam, R. C., Tarling, G. A., and Ward, P.: KRILLBASE: a circumpolar database of Antarctic krill and salp numerical densities, 1926–2016, Earth Syst. Sci. Data, 9, 193–210, https://doi.org/10.5194/essd-9-193-2017, 2017.

Bahlburg, D., Hüppe, L., Böhrer, T., Thorpe, S. E., Murphy, E. J., Berger, U., and Meyer, B.: Plasticity and seasonality of the vertical migration behaviour of Antarctic krill using acoustic data from fishing vessels, R. Soc. Open Sci., 10, https://doi.org/10.1098/rsos.230520, 2023.

Baker, C. A., Estapa, M. L., Iversen, M., Lampitt, R., and Buesseler, K.: Are all sediment traps created equal? An intercomparison study of carbon export methodologies at the PAP-SO site, Prog. Oceanogr., 184, 102317, https://doi.org/10.1016/j.pocean.2020.102317, 2020.

549 Baker, C. A., Martin, A. P., Yool, A., and Popova, E.: Biological Carbon Pump Sequestration
550 Efficiency in the North Atlantic: A Leaky or a Long-Term Sink?, Global Biogeochem. Cycles, 36,
551 https://doi.org/10.1029/2021GB007286, 2022.

552 Balaguer, J., Koch, F., Flintrop, C. M., Völkner, C., Iversen, M. H., and Trimborn, S.: Iron and
553 manganese availability drives primary production and carbon export in the Weddell Sea,
554 Current Biology, 33, 4405-4414.e4, https://doi.org/10.1016/j.cub.2023.08.086, 2023.

555 Bathmann, U., Fischer, G., Moller, P. J., and Gerdes, D.: Short-term variations in particulate
556 matter sedimentation off Kapp Norvegia, Weddell Sea, Antarctica: relation to water mass
557 advection, ice cover, plankton biomass and feeding activity, Polar Biol., 11,
558 https://doi.org/10.1007/BF00240207, 1991.

559 Belcher, A., Tarling, G. A., Manno, C., Atkinson, A., Ward, P., Skaret, G., Fielding, S., Henson, S.
560 A., and Sanders, R.: The potential role of Antarctic krill faecal pellets in efficient carbon export
561 at the marginal ice zone of the South Orkney Islands in spring, Polar Biol., 40, 2001–2013,
562 https://doi.org/10.1007/s00300-017-2118-z, 2017.

563 Belcher, A., Henson, S. A., Manno, C., Hill, S. L., Atkinson, A., Thorpe, S. E., Fretwell, P., Ireland,
564 L., and Tarling, G. A.: Krill faecal pellets drive hidden pulses of particulate organic carbon in the
565 marginal ice zone, Nat. Commun., 10, 889, https://doi.org/10.1038/s41467-019-08847-1, 2019.

566 von Berg, L., Prend, C. J., Campbell, E. C., Mazloff, M. R., Talley, L. D., and Gille, S. T.: Weddell
567 Sea Phytoplankton Blooms Modulated by Sea Ice Variability and Polynya Formation, Geophys.
568 Res. Lett., 47, https://doi.org/10.1029/2020GL087954, 2020.

569 von Bodungen, B.: Phytoplankton growth and krill grazing during spring in the Bransfield Strait,
570 Antarctica — Implications from sediment trap collections, Polar Biol., 6, 153–160,
571 https://doi.org/10.1007/BF00274878, 1986.

572 Boyd, P. W., Arrigo, K. R., Ardyna, M., Halfter, S., Huckstadt, L., Kuhn, A. M., Lannuzel, D.,
573 Neukermans, G., Novaglio, C., Shadwick, E. H., Swart, S., and Thomalla, S. J.: The role of biota in
574 the Southern Ocean carbon cycle, Nat. Rev. Earth Environ., 5, 390–408,
575 https://doi.org/10.1038/s43017-024-00531-3, 2024.

576 de Boyer Montégut, C., Madec, G., Fischer, A. S., Lazar, A., and Iudicone, D.: Mixed layer depth
577 over the global ocean: An examination of profile data and a profile-based climatology, J.
578 Geophys. Res. Oceans, 109, https://doi.org/10.1029/2004JC002378, 2004.

579 Brierley, A. S., Fernandes, P. G., Brandon, M. A., Armstrong, F., Millard, N. W., McPhail, S. D.,
580 Stevenson, P., Pebody, M., Perrett, J., Squires, M., Bone, D. G., and Griffiths, G.: Antarctic Krill
581 Under Sea Ice: Elevated Abundance in a Narrow Band Just South of Ice Edge, Science (1979).,
582 295, 1890–1892, https://doi.org/10.1126/science.1068574, 2002.

583 Briggs, N., Dall'Olmo, G., and Claustre, H.: Major role of particle fragmentation in regulating
584 biological sequestration of CO_2 by the oceans, Science (1979)., 367, 791–793,
585 https://doi.org/10.1126/science.aay1790, 2020.

586 Brown, P. J., Jullion, L., Landschützer, P., Bakker, D. C. E., Naveira Garabato, A. C., Meredith, M.
587 P., Torres-Valdés, S., Watson, A. J., Hoppema, M., Loose, B., Jones, E. M., Telszewski, M., Jones,
588 S. D., and Wanninkhof, R.: Carbon dynamics of the Weddell Gyre, Southern Ocean, Global
589 Biogeochem. Cycles, 29, 288–306, https://doi.org/10.1002/2014GB005006, 2015.

590 Buesseler, K. O., Steinberg, D. K., Michaels, A. F., Johnson, R. J., Andrews, J. E., Valdes, J. R., and
591 Price, J. F.: A comparison of the quantity and composition of material caught in a neutrally
592 buoyant versus surface-tethered sediment trap, Deep Sea Research Part I: Oceanographic
593 Research Papers, 47, 277–294, https://doi.org/10.1016/S0967-0637(99)00056-4, 2000.

594 Buesseler, K. O., Boyd, P. W., Black, E. E., and Siegel, D. A.: Metrics that matter for assessing the
595 ocean biological carbon pump, Proceedings of the National Academy of Sciences, 117, 9679–
596 9687, https://doi.org/10.1073/pnas.1918114117, 2020.

597 Cadee, G. C.: Organic carbon in the upper layer and its sedimentation during the ice-retreat
598 period in the Scotia-Weddell Sea, 1988, Polar Biol., 12, https://doi.org/10.1007/BF00238267,
599 1992.

600 Carlson, C. A., Hansell, D. A., Peltzer, E. T., and Smith, W. O.: Stocks and dynamics of dissolved
601 and particulate organic matter in the southern Ross Sea, Antarctica, Deep Sea Research Part II:
602 Topical Studies in Oceanography, 47, 3201–3225, https://doi.org/10.1016/S0967-
603 0645(00)00065-5, 2000.

604 Cavan, E. L., Le Moigne, F. A. C., Poulton, A. J., Tarling, G. A., Ward, P., Daniels, C. J., Fragoso, G.
605 M., and Sanders, R. J.: Attenuation of particulate organic carbon flux in the Scotia Sea, Southern
606 Ocean, is controlled by zooplankton fecal pellets, Geophys. Res. Lett., 42, 821–830,
607 https://doi.org/10.1002/2014GL062744, 2015.

608 Cavan, E. L., Belcher, A., Atkinson, A., Hill, S. L., Kawaguchi, S., McCormack, S., Meyer, B.,
609 Nicol, S., Ratnarajah, L., Schmidt, K., Steinberg, D. K., Tarling, G. A., and Boyd, P. W.: The
610 importance of Antarctic krill in biogeochemical cycles, Nat. Commun., 10, 4742,
611 https://doi.org/10.1038/s41467-019-12668-7, 2019.

612 Clarke, A. and Tyler, P. A.: Adult Antarctic Krill Feeding at Abyssal Depths, Current Biology, 18,
613 282–285, https://doi.org/10.1016/j.cub.2008.01.059, 2008.

614 Copin-Montegut, C. and Copin-Montegut, G.: Stoichiometry of carbon, nitrogen, and
615 phosphorus in marine particulate matter, Deep Sea Research Part A. Oceanographic Research
616 Papers, 30, 31–46, https://doi.org/10.1016/0198-0149(83)90031-6, 1983.

617 Cozzi, S. and Cantoni, C.: Stable isotope (δ^{13} C and δ^{15} N) composition of particulate organic
618 matter, nutrients and dissolved organic matter during spring ice retreat at Terra Nova Bay,
619 Antarct. Sci., 23, 43–56, https://doi.org/10.1017/S0954102010000611, 2011.

620 Daly, K. L. and Macaulay, M. C.: Abundance and distribution of krill in the ice edge zone of the
621 Weddell Sea, austral spring 1983, Deep Sea Research Part A. Oceanographic Research Papers,
622 35, 21–41, https://doi.org/10.1016/0198-0149(88)90055-6, 1988.

623 DeVries, T.: The Ocean Carbon Cycle, Annu. Rev. Environ. Resour., 47, 317–341,
624 https://doi.org/10.1146/annurev-environ-120920-111307, 2022.

625 Dunbar, R. B.: Sediment trap experiments on the Antarctic continental margin, Antarct. J. US.,
626 19.5, 70–71, 1984.

627 El-Sayed, S. Z. and Taguchi, S.: Primary production and standing crop of phytoplankton along
628 the ice-edge in the Weddell Sea, Deep Sea Research Part A. Oceanographic Research Papers,
629 28, 1017–1032, https://doi.org/10.1016/0198-0149(81)90015-7, 1981.

Freudenthal, T., Neuer, S., Meggers, H., Davenport, R., and Wefer, G.: Influence of lateral particle advection and organic matter degradation on sediment accumulation and stable nitrogen isotope ratios along a productivity gradient in the Canary Islands region, Mar. Geol., 177, 93–109, https://doi.org/10.1016/S0025-3227(01)00126-8, 2001.

George, R. Y. and Stromberg, J.-O.: Development of eggs of Antarctic krill *Euphausia superba* in relation to pressure, Polar Biol., 4, 125–133, https://doi.org/10.1007/BF00263875, 1985.

Goldthwait, S., Carlson, C., Henderson, G., and Alldredge, A.: Effects of physical fragmentation on remineralization of marine snow, Mar. Ecol. Prog. Ser., 305, 59–65, https://doi.org/10.3354/meps305059, 2005.

Guihen, D., Fielding, S., Murphy, E. J., Heywood, K. J., and Griffiths, G.: An assessment of the use of ocean gliders to undertake acoustic measurements of zooplankton: the distribution and density of Antarctic krill (*Euphausia superba*) in the Weddell Sea., Limnol. Oceanogr. Methods, 12, 373–389, https://doi.org/10.4319/lom.2014.12.373, 2014.

Harrington, S. A. and Ikeda, T.: Laboratory observations on spawning, brood size and egg hatchability of the Antarctic krill *Euphausia superba* from Prydz Bay, Antarctica, Mar. Biol., 92, 231–235, https://doi.org/10.1007/BF00392840, 1986.

Hoppe, C. J. M., Klaas, C., Ossebaar, S., Soppa, M. A., Cheah, W., Laglera, L. M., Santos-Echeandia, J., Rost, B., Wolf-Gladrow, D. A., Bracher, A., Hoppema, M., Strass, V., and Trimborn, S.: Controls of primary production in two phytoplankton blooms in the Antarctic Circumpolar Current, Deep Sea Research Part II: Topical Studies in Oceanography, 138, 63–73, https://doi.org/10.1016/j.dsr2.2015.10.005, 2017.

Hoppema, M.: Weddell Sea is a globally significant contributor to deep-sea sequestration of natural carbon dioxide, Deep Sea Research Part I: Oceanographic Research Papers, 51, 1169–1177, https://doi.org/10.1016/j.dsr.2004.02.011, 2004.

Ikeda, T.: Metabolic rate and elemental composition (C and N) of embryos and non-feeding early larval stages of Antarctic krill (*Euphausia superba* Dana), J. Exp. Mar. Biol. Ecol., 90, 119–127, https://doi.org/10.1016/0022-0981(85)90114-5, 1985.

Isla, E., Gerdes, D., Palanques, A., Gili, J.-M., and Arntz, W.: Particle fluxes and tides near the continental ice edge on the eastern Weddell Sea shelf, Deep Sea Research Part II: Topical Studies in Oceanography, 53, 866–874, https://doi.org/10.1016/j.dsr2.2006.02.010, 2006.

Johnson, G. C.: Quantifying Antarctic Bottom Water and North Atlantic Deep Water volumes, J. Geophys. Res. Oceans, 113, https://doi.org/10.1029/2007JC004477, 2008.

Joshi, M., Mestas-Nuñez, A. M., Ackley, S. F., Arndt, S., Macdonald, G. J., and Haas, C.: Seasonal and Interannual Variations in Sea Ice Thickness in the Weddell Sea, Antarctica (2019–2022) Using ICESat-2, Remote Sens. (Basel)., 16, 3909, https://doi.org/10.3390/rs16203909, 2024.

Kennedy, H., Thomas, D., Kattner, G., Haas, C., and Dieckmann, G.: Particulate organic matter in Antarctic summer sea ice: concentration and stable isotopic composition, Mar. Ecol. Prog. Ser., 238, 1–13, https://doi.org/10.3354/meps238001, 2002.

Klunder, M. B., Laan, P., De Baar, H. J. W., Middag, R., Neven, I., and Van Ooijen, J.: Dissolved Fe across the Weddell Sea and Drake Passage: impact of DFe on nutrient uptake, Biogeosciences, 11, 651–669, https://doi.org/10.5194/bg-11-651-2014, 2014.

Lacour, L., Llort, J., Briggs, N., Strutton, P. G., and Boyd, P. W.: Seasonality of downward carbon export in the Pacific Southern Ocean revealed by multi-year robotic observations, Nat. Commun., 14, 1278, https://doi.org/10.1038/s41467-023-36954-7, 2023.

Lannuzel, D., Vancoppenolle, M., van der Merwe, P., de Jong, J., Meiners, K. M., Grotti, M., Nishioka, J., and Schoemann, V.: Iron in sea ice: Review and new insights, Elementa: Science of the Anthropocene, 4, https://doi.org/10.12952/journal.elementa.000130, 2016.

Liszka, C. M., Manno, C., Stowasser, G., Robinson, C., and Tarling, G. A.: Mesozooplankton Community CompositionControls Fecal Pellet Flux and Remineralization Depth in the Southern Ocean, Front. Mar. Sci., 6, https://doi.org/10.3389/fmars.2019.00230, 2019.

Manno, C., Stowasser, G., Enderlein, P., Fielding, S., and Tarling, G. A.: The contribution of zooplankton faecal pellets to deep-carbon transport in the Scotia Sea (Southern Ocean), Biogeosciences, 12, 1955–1965, https://doi.org/10.5194/bg-12-1955-2015, 2015.

Manno, C., Fielding, S., Stowasser, G., Murphy, E. J., Thorpe, S. E., and Tarling, G. A.: Continuous moulting by Antarctic krill drives major pulses of carbon export in the north Scotia Sea, Southern Ocean, Nat. Commun., 11, 6051, https://doi.org/10.1038/s41467-020-19956-7, 2020.

Manno, C., Stowasser, G., Fielding, S., Apeland, B., and Tarling, G. A.: Deep carbon export peaks are driven by different biological pathways during the extended Scotia Sea (Southern Ocean) bloom, Deep. Sea. Res. 2. Top. Stud. Oceanogr., 205, https://doi.org/10.1016/j.dsr2.2022.105183, 2022.

Manno, C., Corsi, I., Rowlands, E., and Bergami, E.: Plastics counteract the ability of Antarctic krill to promote the blue carbon pathway in the deep ocean, Mar. Pollut. Bull., 209, 117238, https://doi.org/10.1016/j.marpolbul.2024.117238, 2024.

Martin, J. H., Knauer, G. A., Karl, D. M., and Broenkow, W. W.: VERTEX: carbon cycling in the northeast Pacific, Deep Sea Research Part A. Oceanographic Research Papers, 34, 267–285, https://doi.org/10.1016/0198-0149(87)90086-0, 1987.

Mayor, D. J., Sanders, R., Giering, S. L. C., and Anderson, T. R.: Microbial gardening in the ocean's twilight zone: Detritivorous metazoans benefit from fragmenting, rather than ingesting, sinking detritus, BioEssays, 36, 1132–1137, https://doi.org/10.1002/bies.201400100, 2014.

Michels, J., Dieckmann, G. S., Thomas, D. N., Schnack-Schiel, S. B., Krell, A., Assmy, P., Kennedy, H., Papadimitriou, S., and Cisewski, B.: Short-term biogenic particle flux under late spring sea ice in the western Weddell Sea, Deep Sea Research Part II: Topical Studies in Oceanography, 55, 1024–1039, https://doi.org/10.1016/j.dsr2.2007.12.019, 2008.

Middag, R., de Baar, H. J. W., Klunder, M. B., and Laan, P.: Fluxes of dissolved aluminium and manganese to the Weddell Sea and indications for manganese co-limitation, Limnol. Oceanogr., 58, 287–300, https://doi.org/10.4319/lo.2013.58.1.0287, 2013.

Le Moigne, F. A. C.: Pathways of Organic Carbon Downward Transport by the Oceanic Biological Carbon Pump, Front. Mar. Sci., 6, https://doi.org/10.3389/fmars.2019.00634, 2019.

Le Moigne, F. A. C., Poulton, A. J., Henson, S. A., Daniels, C. J., Fragoso, G. M., Mitchell, E., Richier, S., Russell, B. C., Smith, H. E. K., Tarling, G. A., Young, J. R., and Zubkov, M.: Carbon export efficiency and phytoplankton community composition in the Atlantic sector of the Arctic

711 Ocean, J. Geophys. Res. Oceans, 120, 3896–3912, https://doi.org/10.1002/2015JC010700,
712 2015.

713 Mouw, C. B., Barnett, A., McKinley, G. A., Gloege, L., and Pilcher, D.: Global ocean particulate
714 organic carbon flux merged with satellite parameters, Earth Syst. Sci. Data, 8, 531–541,
715 https://doi.org/10.5194/essd-8-531-2016, 2016.

716 Niemi, A. and Michel, C.: Temporal and spatial variability in sea-ice carbon:nitrogen ratios on
717 Canadian Arctic shelves, Elementa: Science of the Anthropocene, 3,
718 https://doi.org/10.12952/journal.elementa.000078, 2015.

719 Nissen, C., Timmermann, R., Hoppema, M., Gürses, Ö., and Hauck, J.: Abruptly attenuated
720 carbon sequestration with Weddell Sea dense waters by 2100, Nat. Commun., 13, 3402,
721 https://doi.org/10.1038/s41467-022-30671-3, 2022.

722 Orsi, A. H., Johnson, G. C., and Bullister, J. L.: Circulation, mixing, and production of Antarctic
723 Bottom Water, Prog. Oceanogr., 43, 55–109, https://doi.org/10.1016/S0079-6611(99)00004-X,
724 1999.

725 Pauli, N.-C., Flintrop, C. M., Konrad, C., Pakhomov, E. A., Swoboda, S., Koch, F., Wang, X.-L.,
726 Zhang, J.-C., Brierley, A. S., Bernasconi, M., Meyer, B., and Iversen, M. H.: Krill and salp faecal
727 pellets contribute equally to the carbon flux at the Antarctic Peninsula, Nat. Commun., 12,
728 7168, https://doi.org/10.1038/s41467-021-27436-9, 2021.

729 Perhirin, M., Aumont, O., Maps, F., and Ayata, S.-D.: Meta-analysis of the role of zooplankton
730 faecal pellets in ocean carbon export flux, ICES Journal of Marine Science, 82,
731 https://doi.org/10.1093/icesjms/fsaf180, 2025.

732 Perry, F. A., Kawaguchi, S., Atkinson, A., Sailley, S. F., Tarling, G. A., Mayor, D. J., Lucas, C. H.,
733 King, R., and Cooper, A.: Temperature–Induced Hatch Failure and Nauplii Malformation in
734 Antarctic Krill, Front. Mar. Sci., 7, https://doi.org/10.3389/fmars.2020.00501, 2020.

735 Pudsey, C. J. and King, P.: Particle fluxes, benthic processes and the palaeoenvironmental
736 record in the Northern Weddell Sea, Deep Sea Research Part I: Oceanographic Research
737 Papers, 44, 1841–1876, https://doi.org/10.1016/S0967-0637(97)00064-2, 1997.

738 Quetin, L. B. and Ross, R. M.: Environmental Variability and Its Impact on the Reproductive
739 Cycle of Antarctic Krill, Am. Zool., 41, 74–89, https://doi.org/10.1093/icb/41.1.74, 2001.

740 Redfield, A. C.: On the Proportions of Organic Derivatives in Sea Water and Their Relation to the
741 Composition of Plankton., James Johnstone Memorial Volume, University Press of Liverpool,
742 176-192., 1934.

743 Richter, M. E., Zheng, Y., Nicholls, K., Boehme, L., McAfee, C., Singh, C., Bell, T., & Heywood, K.
744 (2026). CTD data near floating sediment trap deployments on the western Weddell Sea
745 continental shelf during early 2024 (1.0.0). Zenodo, https://doi.org/10.5281/zenodo.20849254

746 Robinson, C., Serret, P., Tilstone, G., Teira, E., Zubkov, M. V, Rees, A. P., and Woodward, E. M. S.:
747 Plankton respiration in the Eastern Atlantic Ocean, Deep Sea Research Part I: Oceanographic
748 Research Papers, 49, 787–813, https://doi.org/10.1016/S0967-0637(01)00083-8, 2002.

749 Salyuk, P. A., Glukhovets, D. I., Latushkin, A. A., Kalinina, O. Yu., Shtraikhert, E. A., Sapozhnikov,
750 P. V., Mosharov, S. A., Stepochkin, I. E., Lipinskaya, N. A., Gorbov, M. I., and Klimenko, S. K.:
751 Extreme underestimation of satellite-derived chlorophyll-a concentration in the northwestern

Weddell Sea during a phytoplankton bloom and its reasons, Journal of Marine Systems, 252, 104159, https://doi.org/10.1016/j.jmarsys.2025.104159, 2025.

Schmidt, K., Atkinson, A., Steigenberger, S., Fielding, S., Lindsay, M. C. M., Pond, D. W., Tarling, G. A., Klevjer, T. A., Allen, C. S., Nicol, S., and Achterberg, E. P.: Seabed foraging by Antarctic krill: Implications for stock assessment, bentho-pelagic coupling, and the vertical transfer of iron, Limnol. Oceanogr., 56, 1411–1428, https://doi.org/10.4319/lo.2011.56.4.1411, 2011.

Schmidt, K., Brown, T. A., Belt, S. T., Ireland, L. C., Taylor, K. W. R., Thorpe, S. E., Ward, P., and Atkinson, A.: Do pelagic grazers benefit from sea ice? Insights from the Antarctic sea ice proxy $IPSO_{25}$, Biogeosciences, 15, 1987–2006, https://doi.org/10.5194/bg-15-1987-2018, 2018.

Semper, S. and Darelius, E.: Seasonal resonance of diurnal coastal trapped waves in the southern Weddell Sea, Antarctica, Ocean Science, 13, 77–93, https://doi.org/10.5194/os-13-77-2017, 2017.

Smith, A. J. R., Wotherspoon, S., Ratnarajah, L., Cutter, G. R., Macaulay, G. J., Hutton, B., King, R., Kawaguchi, S., and Cox, M. J.: Antarctic krill vertical migrations modulate seasonal carbon export, Science (1979)., 387, https://doi.org/10.1126/science.adq5564, 2025.

Smith, K. L., Ruhl, H. A., Huffard, C. L., Messié, M., and Kahru, M.: Episodic organic carbon fluxes from surface ocean to abyssal depths during long-term monitoring in NE Pacific, Proceedings of the National Academy of Sciences, 115, 12235–12240, https://doi.org/10.1073/pnas.1814559115, 2018.

Smith, W. O. and Nelson, D. M.: Phytoplankton Bloom Produced by a Receding Ice Edge in the Ross Sea: Spatial Coherence with the Density Field, Science (1979)., 227, 163–166, https://doi.org/10.1126/science.227.4683.163, 1985.

Spreen, G., Kaleschke, L., and Heygster, G.: Sea ice remote sensing using AMSR-E 89-GHz channels, J. Geophys. Res. Oceans, 113, https://doi.org/10.1029/2005JC003384, 2008.

Steinberg, D. K. and Landry, M. R.: Zooplankton and the Ocean Carbon Cycle, Ann. Rev. Mar. Sci., 9, 413–444, https://doi.org/10.1146/annurev-marine-010814-015924, 2017.

Steinke, K. B., Bernard, K. S., Reiss, C. S., Walsh, J., Correa, G. M., and Stammerjohn, S. E.: Factors impacting the timing of reproductive development in female Antarctic krill at the northwestern Antarctic Peninsula, Front. Mar. Sci., 11, https://doi.org/10.3389/fmars.2024.1383175, 2024.

Tanioka, T., Garcia, C. A., Larkin, A. A., Garcia, N. S., Fagan, A. J., and Martiny, A. C.: Global patterns and predictors of C:N:P in marine ecosystems, Commun. Earth Environ., 3, 271, https://doi.org/10.1038/s43247-022-00603-6, 2022.

Tarling, G. A., Thorpe, S. E., Fielding, S., Klevjer, T., Ryabov, A., and Somerfield, P. J.: Varying depth and swarm dimensions of open-ocean Antarctic krill *Euphausia superba* Dana, 1850 (Euphausiacea) over diel cycles., Journal of Crustacean Biology, 38, 1–12, 2018.

Trinh, R., Ducklow, H. W., Steinberg, D. K., and Fraser, W. R.: Krill body size drives particulate organic carbon export in West Antarctica, Nature, 618, 526–530, https://doi.org/10.1038/s41586-023-06041-4, 2023.

Turner, J. T.: Zooplankton fecal pellets, marine snow, phytodetritus and the ocean's biological pump, Prog. Oceanogr., 130, 205–248, https://doi.org/10.1016/j.pocean.2014.08.005, 2015.

Volk, T. and Hoffert, M. I.: The Carbon cycle and atmospheric CO_2: natural variations, Archean to present, edited by: Sundquist, E. T. and Broecker, W. S., American Geophysical Union, 627 pp., 1985.

Wakeham, S. G., Lee, C., Hedges, J. I., Hernes, P. J., and Peterson, M. J.: Molecular indicators of diagenetic status in marine organic matter, Geochim. Cosmochim. Acta, 61, 5363–5369, https://doi.org/10.1016/S0016-7037(97)00312-8, 1997.

Wefer, G., Fischer, G., Fütterer, D. K., Gersonde, R., Honjo, S., and Ostermann, D.: Particle Sedimentation and Productivity in Antarctic Waters of the Atlantic Sector, in: Geological History of the Polar Oceans: Arctic versus Antarctic, Springer Netherlands, Dordrecht, 363–379, https://doi.org/10.1007/978-94-009-2029-3_20, 1990.

Whitehouse, M., Atkinson, A., Ward, P., Korb, R., Rothery, P., and Fielding, S.: Role of krill versus bottom-up factors in controlling phytoplankton biomass in the northern Antarctic waters of South Georgia, Mar. Ecol. Prog. Ser., 393, 69–82, https://doi.org/10.3354/meps08288, 2009.

Wilkinson B. (2026). Chlorophyll-a samples collected in the Southern Ocean on cruise SD035 in January-March 2024 as part of PICCOLO. NERC EDS British Oceanographic Data Centre NOC. doi:10.5285/4f7aed48-816a-d8cf-e063-7086abc055b4

Yoshida, T., Virtue, P., Kawaguchi, S., and Nichols, P. D.: Factors determining the hatching success of Antarctic krill *Euphausia superba* embryo: lipid and fatty acid composition, Mar. Biol., 158, 2313–2325, https://doi.org/10.1007/s00227-011-1735-2, 2011.